Understanding ageing mechanism of carbon electrodes in double layer capacitors operating in organic electrolytes

Elodie Marcerou, Barbara Daffos, Pierre-Louis Taberna, Patrice Simon

Understanding Ageing Mechanism of Carbon Electrodes in Double Layer Capacitors Operating in Organic Electrolytes

Elodie Marcerou[1], Barbara Daffos[1,2], Pierre-Louis Taberna[1,2] and Patrice Simon[1,2]

[1]CIRIMAT, Université Toulouse III, Paul Sabatier
[2]Réseau sur le Stockage Electrochimique de l'Energie (RS2E), FR CNRS 3459, 80039 Amiens Cedex, France

Corresponding author: Patrice Simon, patrice.simon@univ-tlse3.fr

Highlights :

Aging of supercapacitors with two different carbons is studied through different methods

two different ageing mechanism are observed because of the differences on carbons (porosity, surface state, etc)

Polymerization film on YP50F positive electrode, more defect density for CMK3 positive electrode

Keywords :

Supercapacitors ageing

Carbon materials

Ageing mechanisms

Funding source:

This work was supported by the French national agency of research (ANR).

ABSTRACT

Understanding the ageing mechanisms of porous carbon electrodes used in electrochemical double layers supercapacitors (EDLCs) is of high importance to improve their lifetime. In this work, we studied ageing of two different porous carbons with different pore size distribution and surface functionalities in 1.5 M tetraethyl ammonium tetrafluoroborate (Et_4NBF_4) in acetonitrile (AN) electrolyte. The combination of Raman spectroscopy, thermogravimetric analysis (TGA), gas sorption and electrochemical impedance spectroscopy techniques allowed us to identify two different behaviors depending on the porous carbon used. A microporous carbon experiences an ionic/electronic resistance increase leading to a capacitance fall off upon cycling, associated with pore clogging. This resulted from the electrolyte degradation taking place at the positive electrode combined with porous carbon oxidation. Differently, only an increase of the series resistance was observed for the mesoporous carbon tested, following the creation of defects at the positive carbon electrode.

INTRODUCTION

Electrochemical double layer capacitors (EDLCs) are electrochemical energy storage devices used for fast charge/discharge applications. Differently from batteries, they can deliver high power but suffer from limited energy density (about 10Wh/kg compared to 250 Wh/kg for Li-ion batteries (LIBs))[1].

EDLCs store the charge by electrostatic adsorption of ions from the electrolyte onto high surface area porous carbons (about 2,000 m^2g^{-1})[2]. It has been reported that the pore size and pore size distribution have a tremendous influence on Supercapacitors (SCs) performances. While nanopores favor high capacitance performance — maximum capacitance can be achieved when the pore size is near to the ion size[3,4] — mesoporosity favors fast ion transport within the carbon porous network[5]. Thus, the study of activated carbons with different Pore Size Distribution (PSD) could help bringing insights to better understand ageing mechanisms. Even though they can endure millions of cycles, EDLCs suffer from ageing during operation and more specifically during operation at high potential, that result in capacitance loss and resistance increase. Although those ageing mechanisms are still not fully understood, various hypothesis have been proposed in the literature. Hahn et al. have shown that, during voltage hold experiments, a part of the leakage current leads to gas formation and thus to an irreversible inner pressure increase of the cell in propylene carbonate based electrolytes[6]. Thanks to a Differential Electrochemical Mass Spectroscopy (DEMS) analysis, they identified CO_2 as the main degradation product, together with propene and H_2, the former being related to both solvent and carbon oxidation at the positive electrode and the latter from the solvent reduction at the negative electrode. Recently, Pameté and al.[7] focused specifically on the degradation of electrolytes caused by elevated voltage and/or temperatures during cycling. They presented a comprehensive summary of well-documented failure mechanisms, including the formation of gases or solid byproducts that have the potential to obstruct the pores.

Parasitic degradation reactions occuring at the electrode/electrolyte interface are expected to be strongly correlated to the carbon surface morphology and chemistry. Accordingly, the so-called activation (oxidation) process used to prepare high surface area carbon[8] play an important role as this process modifies the carbon surface chemistry and porous structure which in turn affects the charge storage mechanism and the electrode ageing kinetic[9]. For instance, it was shown that the presence of oxygen-containing acidic functional groups on carbon participate to the cell degradation[10,11]. Yang et al. reported that carboxyl, lactone and phenol groups onto the surface of carbons lead to high leakage current and gas evolution[12]. In 2021, Pourhosseini et al.[13] showed that the positive carbon electrode could have a 4wt.% increase in the oxygen content after ageing during positive polarization, while electrode functionalities

were transformed to more thermally stable functions (from acidic carboxylic to lactone and carbonyl type functionalities) during negative polarization.

Thus, various carbon surface chemistry result in different electrolyte/material interaction and ageing mechanism.

Electrolyte impurities such as water in non-aqueous electrolytes are also a cause of capacitance loss by water electrolysis and further carbon oxidation[14]; electrochemical reactions of non-aqueous solvent can also lead to the formation of polymeric films onto the porous carbon surface[15]. Zhu et al. in 2008[16] reported about the presence of C-H bonds on cathode and C-N and C-F bonds on the carbon negative electrode that could be associated with the polymerization of the acetonitrile solvent. Moreover, different degradation processes were reported for the same material but operating with different electrolytes. Tokita and al. have cycled several EDLCs with various electrolytes upon different cut-off voltages during constant current charge-discharge cycling. They found that EDLC cells were more stable when using acetonitrile-based versus carbonate-based electrolytes. Moreover, they also compared two salts, $LiBF_4$ and Et_4NBF_4 and showed that Et_4NBF_4 containing electrolyte could sustain higher potential (up to 3.5V) in acetonitrile solvent ($1mol.dm^{-3}$).

According to those works, ageing of the EDLC electrodes is related to the electrode / electrolyte interface and thus is strongly dependent on the carbon surface chemistry, carbon porous structure in relationship with the nature of the electrolyte.

In this work, we studied the ageing mechanism of two porous carbons with different pore size and pore size distribution in acetonitrile-based electrolyte during electrochemical tests. Ageing mechanism analysis was performed by combining electrochemical characterization techniques and material characterization techniques such as thermogravimetric analysis, Raman spectroscopy, gas sorption measurements, Boehm titration and IsoElectric Point (IEP) measurement. We were able to observe two different degradation mechanisms depending on the carbon, that gives a better picture of the role of pore size and carbon surface chemistry on the ageing mechanisms of carbon electrodes of EDLCs during operation.

EXPERIMENTAL

- *Electrochemical characterization*

Two different commercial porous carbons were used in this study: CMK3 and YP50F. CMK3 (ACS material, CAS 7440-44-0) is a commercial porous carbon made by impregnation of a SHA-15 silica hard template with sucrose precursor; porous carbon with 3 nm pore size is obtained after further carbonization treatment of the sucrose and SHA-15 dissolution[17]. YP50F (Kuraray Chemicals)[18] is a microporous carbon from natural precursor which is used in commercial supercapacitors[19] with 90% of the pore size below 2 nm (c.f. *supplementary information figure S1 and table S1*).

A free-standing film was made by rolling 95wt% of activated carbon and 5wt% of PolyTetraFluoroEthylene (PTFE, DuPont, France) as binder mixed in ethanol. After 24h in oven at 80°C, electrodes of 8mm diameter were punched from the film (mass loading 6 $mg.cm^{-2}$). 3/8'' Swagelok® cells were assembled using two 8 mm diameter platinum discs as current collector, to ensure a low current collector/activated carbon contact impedance. Platinum has been chosen instead of Al foil, the material commonly used in commercial SCs, to avoid any corrosion or current collector passivation contribution. The separator was a 50µm thick cellulose membrane (Nippon Kodoshi Corporation NKK, type TF4425) and the electrolyte was 1.5M of tetraethylammonium tetrafluoroborate salt (Et_4NBF_4, ACROS Organic™, 99%) dissolved in acetonitrile (AN, ACROS Organic™). The cell assembly was made in a glove box (Jacomex, France) with a purified atmosphere (<1ppm O_2 and <1ppm H_2O).

Electrochemical Impedance Spectroscopy (EIS), Cyclic Voltammetry (CV), Galvanostatic Cycling (GC) and floating were made with a VMP3 potentiostat (Bio-Logic, France). EIS was performed with a 5mV rms sinusoidal signal from 200kHz to 10mHz. The applied ageing protocol has been previously described[20]. Briefly, each cell was tested using a cycle procedure, where one cycle consists in a sequence of 6 GC followed by 12 h floating at 2.7V. The ageing ended when 80 cycles have been done. The capacitance, resistance, current loss and irreversible charge loss were tracked during the ageing. The capacitance and resistance were measured at each sixth GC. It is worth mentioning the equivalent series resistance was measured at a sampling time of 600µs (1667Hz). The leakage current was measured at the very end of each floating step - it was averaged over the last 100 seconds of the floating steps. The irreversible capacity was calculated from the full current integration during the cycle (equation 1).

$$Q_{irr}(t) = \int_0^t i(t)dt \qquad (1)$$

Where $Q_{irr}(t)$ represent the irreversible charge (mA.h), i(t) current (mA).

Indeed, if there is no irreversible capacity, the total integrated current would be null.

Initial and final electrochemical behavior were compared with EIS and CV measurement, before and after ageing. Material characterization were also carried out before and after ageing.

- *Material characterization*

After ageing, electrodes have been extracted from the cell and add in the solvent (ACN) for 72 hours. Then they were store in a 80°C oven.

Porous carbons ware characterized by gas sorption at the liquid nitrogen temperature (77 K) using argon gas with an ASAP 2020 Micromeritics equipment. DFT method was used to calculate the specific surface area (SSA) and to obtain the pore size distribution and the mean pore diameter.

Raman spectroscopy measurements (Xplora, from HORIBA Company) were made on electrodes before and after ageing (positive and negative electrodes). Each time, different areas of the electrodes were analyzed. Spectra were obtained with a green laser (532nm), 1800 tr.min^{-1} and a 50x objective.

Thermogravimetric (TGA) measurements were performed on all the electrodes, before and after ageing. Samples were studied in air atmosphere, from room temperature (20°C) to 1000°C with a gas flow of 40mL min^{-1} and a heating rate of 5°C min^{-1}. Those measurements were achieved with TGA 92-16.18 from SETARAM.

The analysis of the IsoElectric Point (IEP) aims to measure the pH at which the carbon surface has a net zero surface charge. Solutions of 0.01M NaCl at different pH have been prepared (pH_0), the pH have been adjusted with small amount of NaOH or HCl. Carbon powder have been added (pH_i), after 12h of stirring the pH have been measured again (pH_f).

RESULTS AND DISCUSSION

Figure 1 shows the change of the capacitance (F/g) and the resistance (Ω.cm²) versus the number of ageing cycles, for both carbons YP50F and CMK3—80 ageing cycles were applied. As observed, for the same number of ageing cycles, the YP50F carbon experiences a higher capacitance fall-off, -42% while 26% are lost for CMK3. Moreover, the resistance increases a lot more for YP50F (+111%) than the CMK3's one (+46%). Interestingly, it is worth noting in both cases the capacitance decreases monotonically with the cumulative capacity (Q_{irr}) (*c.f. supplementary information, Figure S2)*. According to those results, the cell degradation is strongly correlated to the irreversible cumulative capacity, which was somehow expected[21]. Indeed, even though the total Q_{irr} is twice as high after 80 ageing cycles for YP50F than CMK3 (15 Ah/g vs 6 Ah/g), the mean capacitance variation with Q_{irr} is very close for both carbons: -4.2% / Ah / g. The calculated irreversible cumulative capacity being highly likely connected to parasitic faradic reactions occurring at the electrode/electrolyte interface, the capacitance and resistance variations could be caused by faradic reactions occurring during the high voltage floating steps, which is an indication that the electrolyte and/or the activated carbons are oxidized and/or reduced. Thus, the higher ageing rate observed for YP50F may be due to the presence of functional groups at its surface.

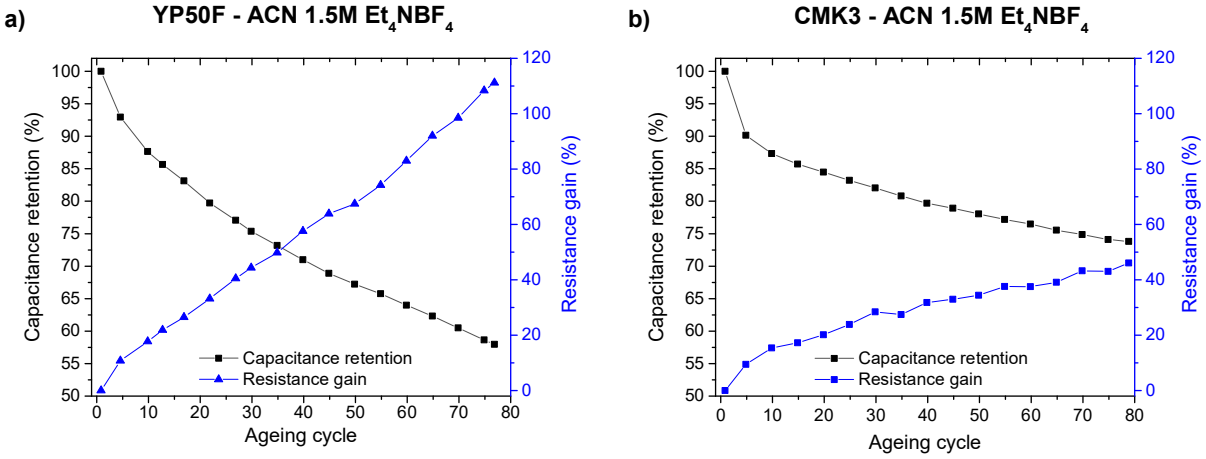

Figure 1: Electrochemical performances evolution during the ageing. Change of the capacitance and resistance versus cycles for YP50F (a) and CMK3 (b) in AN 1.5M Et_4NBF_4. With C_0(YP50F) = 96 F/g, C_0(CMK3) = 72 F/g, R_0(YP50F) = 1.0 Ω.cm², R_0(CMK3) = 0.8 Ω.cm².

Moving further, electrochemical impedance spectroscopy (EIS) measurements were performed for both cells, before and after ageing and their Nyquist plots are shown in Figures 2a and 2b.

YP50F-based cell shows an overall sloping change of Z'' vs Z' (Figure 2a); the high frequency insert evidences the presence of a loop after ageing. Those observations are consistent with an increase of the electrode ionic resistance – corresponding to the electrolyte confined in the carbon porosity and between the carbon grains — although an increase of the electronic resistance of the carbon could also contribute. However, the similar high frequency value (at Z"=0) of the resistance evidences that, if the electronic conductivity of the bulk carbon grains is affected, this should not be the main origin of the presence of the high frequency loop, that can be then ascribed to a rise of the ionic resistance in the porous network of the carbon electrodes[22].This well agrees with previous results that reported preferred ionic path at high frequency[23]. On the other hand, the impedance of CMK3-based cell does not change that much overall but the high frequency resistance as only the real part of the impedance is shifted toward higher values, which may indicate that only the carbon electronic resistance has increased upon ageing.

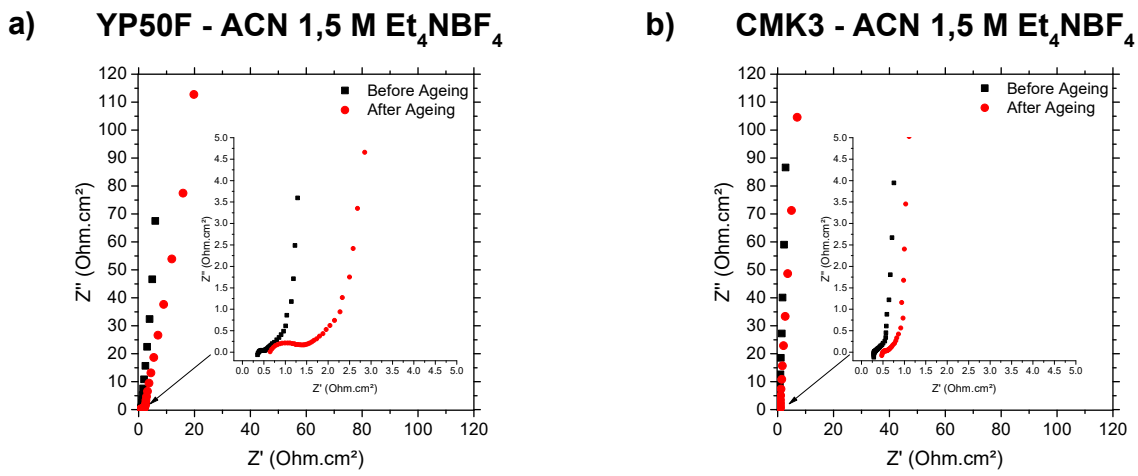

Figure 2: Electrochemical performances evolution before and after the ageing. (2a) and (2b) shows Nyquist plots before and after ageing, respectively for YP50F and CMK3 in acetonitrile 1.5M Et_4NBF_4 with a zoom at high frequencies.

To sum up, YP50F faces important capacitance fading during ageing vs CMK3 (Fig 1a, 1b). Both materials show different impedance behaviors (Fig 2a,2b), suggesting different ageing mechanisms with i) an increase of the carbon ionic-electronic resistance for YP50F-based electrodes, possibly due to the presence degradation products from the electrolyte and/or carbon oxidation[15] and ii) a carbon degradation leading to an increase of the electronic resistance[22] for CMK3-based electrodes.

To get a better understanding about degradation mechanisms that occurs inside those cells, additional material characterization techniques were used.

Gas sorption measurements on raw carbon powders (see in *supplementary information, Figure S1 and Table S1*) revealed higher SSA for YP50F than CMK3 (respectively 1732 m^2/g and 1134 m^2/g). Figure 3 shows the gas sorption isotherms of the YP50F and CMK3 electrodes before (Fig. 3a, 3b) and after ageing of the negative (Fig. 3c, 3d) and positive electrode (Fig. 3e, 3f). As expected for a mesoporous carbon, CMK3 exhibit a type IV isotherm with a hysteresis (Fig. 3a, 3c, 3e). For both carbons, it is worth noting a drastic drop of the total adsorbed volume for the positive electrodes, from 830 m^2/g to 155 m^2/g and 1412 m^2/g to 493 m^2/g for the CMK3 and YP50F, respectively. Differently, the negative electrodes porous volume was kept roughly the same: from 830 m^2/g to 664 m^2/g and 1412 m^2/g to 1326 m^2/g, respectively for CMK3 and YP50F (Fig. 3e, 3f). These measurements agree with previous result reported in the litterature[21,24] showing that the negative electrode is less affected by the ageing compared to the positive as a result of more cathodic polarization. The important loss of porous surface at the positive electrode for both carbons could be consistent with pore clogging by degradation products and/or functional groups or carbon oxidation.

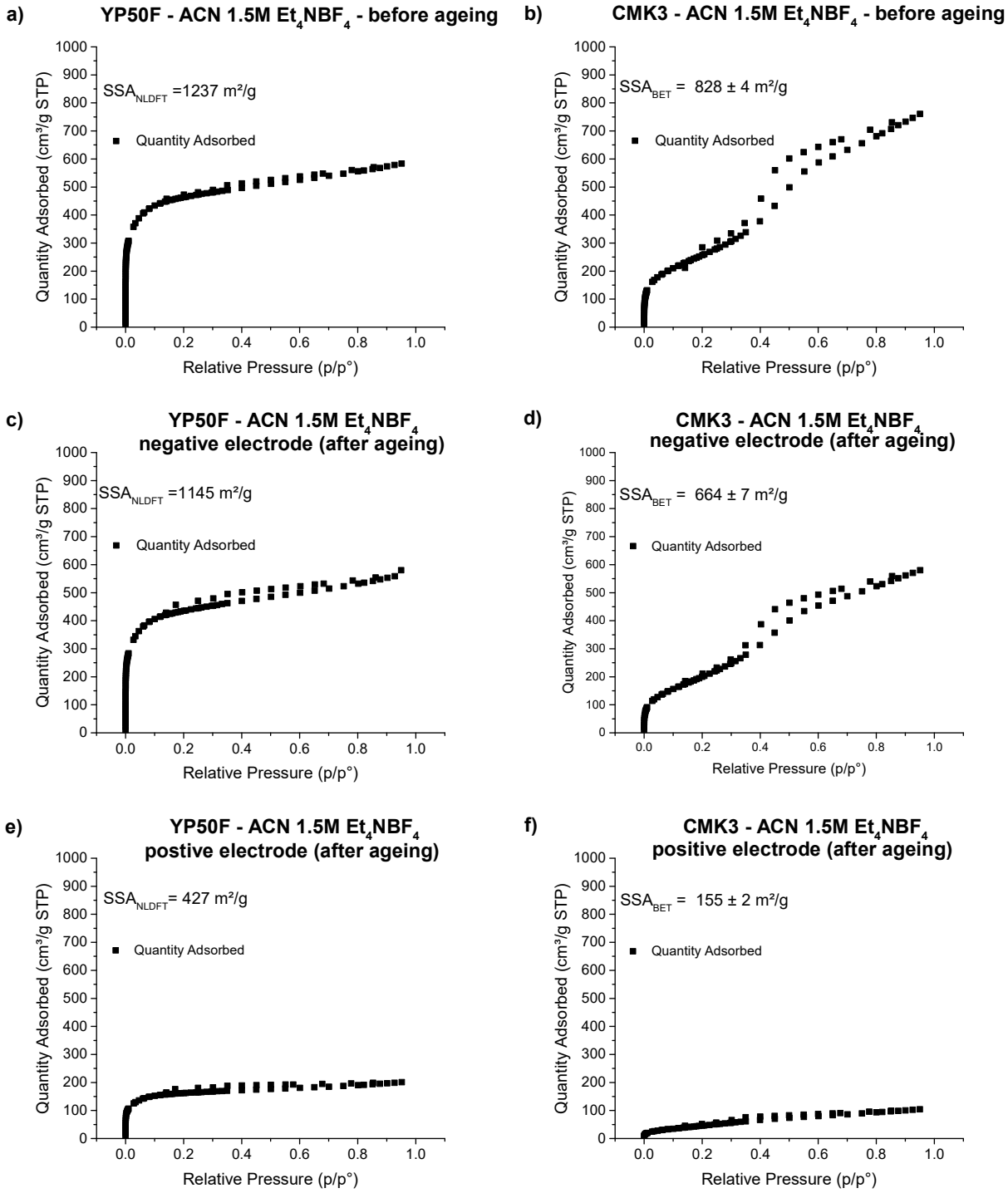

Figure 3: Gas sorption isotherms for both materials electrodes before and after ageing. Quantity of gas adsorbed versus the relative gas pressure for YP50F (a) before ageing electrode, (c) negative electrode, (e) positive electrode and for CMK3 (b) before ageing electrode, (d) negative electrode and (f) positive electrode.

Figure S3 (*see Supplementary Information*) represent the SSA evolution of the aged electrodes and before ageing electrode. Figure S4 (*see Supplementary Information*) shows the distribution of the microporous (< 2 nm pore size) and mesoporous (between 2 and 50 nm pore size) volumes for the positive and negative electrodes, before and after ageing. Both positive electrodes show a decrease in the porous volume and surface area. More specifically, the microporous volume of YP50F positive electrode has vanished after electrochemical ageing, suggesting that the microporosity becomes inaccessible to gas. This observation may suggest the polymerization of a film caused by reactions between the electrolyte and the carbon surface functions, blocking the pore accessibility. CMK3 carbon does not have microporosity but experiences also a drastic porous volume decrease on the positive electrode; a slight variation is observed for the negative electrode. Those findings suggest a change of the porous structure upon ageing but since the impedance was only shifted to higher resistance for the CMK3 porous carbon electrodes, it may be more in line with a structural change of the carbon instead of the formation of polymeric layer from the degradation of the electrolyte.

Raw and aged electrodes were further analyzed ty TGA. Figure 5 shows the derivative of the TGA plots for all the carbon electrodes before and after aging, where the main peak observed around 550°C corresponds to the carbon oxidation (TGA thermogram are in *supplementary information, Figure S5*).

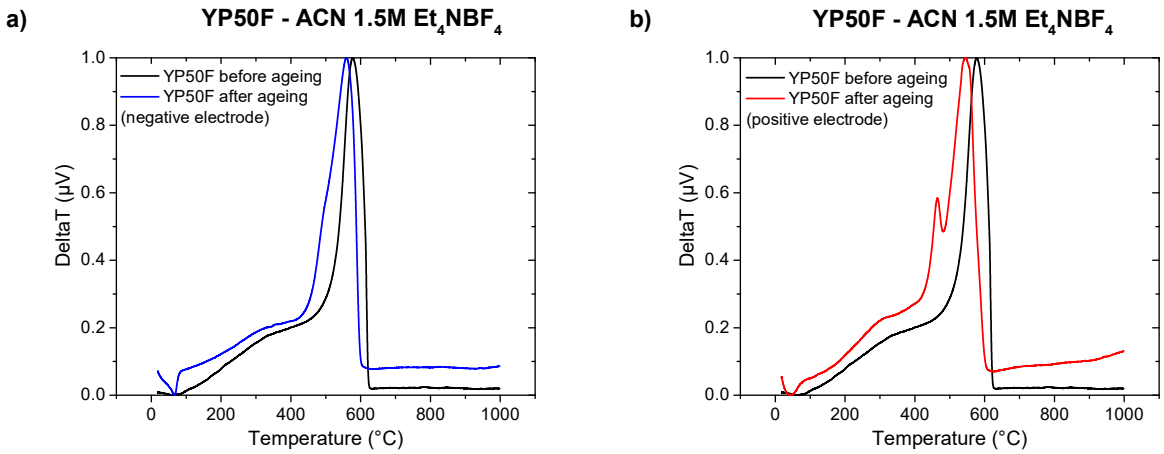

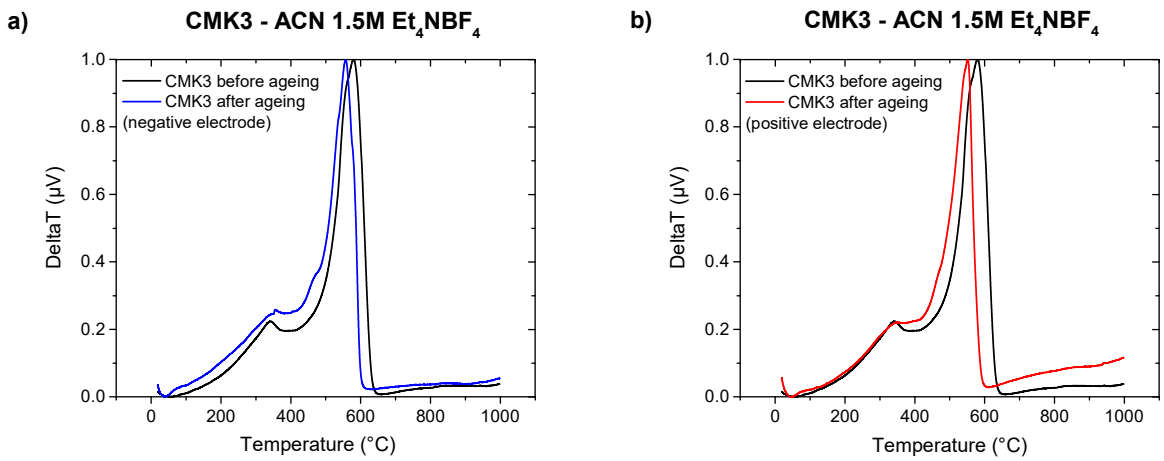

Figure 5: Derivative thermogravimetric plots of (a) YP50F before ageing electrode and negative electrode, (b) YP50F before ageing electrode and positive electrode, (c) CMK3 before ageing electrode and negative electrode, (d) CMK3 before ageing electrode and positive electrode.

All aged electrodes show a lower degradation temperature, compared to raw carbon material—it suggesting that aged electrodes experienced a partial oxidation. However, the shift of the peak temperature for the positive aged electrodes (Fig 5b and 5d) is more pronounced than that of negatives ones (Fig 5a and 5c), that could be consistent with a more oxidized carbon when used as positive electrodes. YP50F positive electrode (Fig 5d) shows an additional degradation peak at 464°C compared to YP50F negative electrode (Figure 5c), in agreement with an increased number of carbon reactive sites, possibly being a group of surface function[25] or carbon surface defects[26] that degrade before the bulk material. Difference in the thermal behavior of YP50F negative and positive electrodes highlights the dependence of degradation mechanism with the electrode potential (anodic or cathodic polarization).

Differently, the CMK3 negative electrode (Figure 5a) and positive electrode (Figure 5c) show similar degradation process with only one main degradation peak. Both electrodes present a slight temperature peak shift that may due to some carbon degradation.

Raman spectra before and after ageing of CMK3 and YP50F electrodes are shown in Figure 6a and 6b, respectively. The two main peaks centered at 1350 cm^{-1} and 1580cm^{-1} correspond to the D and G bands, respectively. Since a perfect graphitic carbon does not have any D peak[27], the I_D/I_G ratio informs about the defect density of the material. Previous results have shown that when the distance between defects L_D is superior to 2nm, the sole use of the I_D/I_G peak ratio become irrelevant to estimate the defect

density[28]. Since our material exhibit broad second order peaks (*Supplementary Information, Figure S6*), we can assume that CMK3 and YP50F carbons have a $L_D > 2nm$.

Besides, as the full width at half maximum of D peak (Γ_{FWHM}) scales inversely with L_D[28], Γ_{FWHM} is another indicator that can be used to assess the defect density of carbon materials. Finally, the intensity between the two peaks, at 1500cm^{-1}, increase when the carbon is more desordered[11,29].

There is no obvious change in the Raman spectra of the YP50F electrode before and after ageing (Figure 6a), with similar Γ_{FWHM}(D) values are measured (Table 1). Differently, the Raman signature of the CMK3 (Figure 6b) positive electrode has a higher peak intensity at 1500cm^{-1}, in the interband region, and a higher Γ_{FWHM} (177 cm^{-1}) versus fresh electrode (145 cm^{-1}), while no change is observed at the negative electrode.

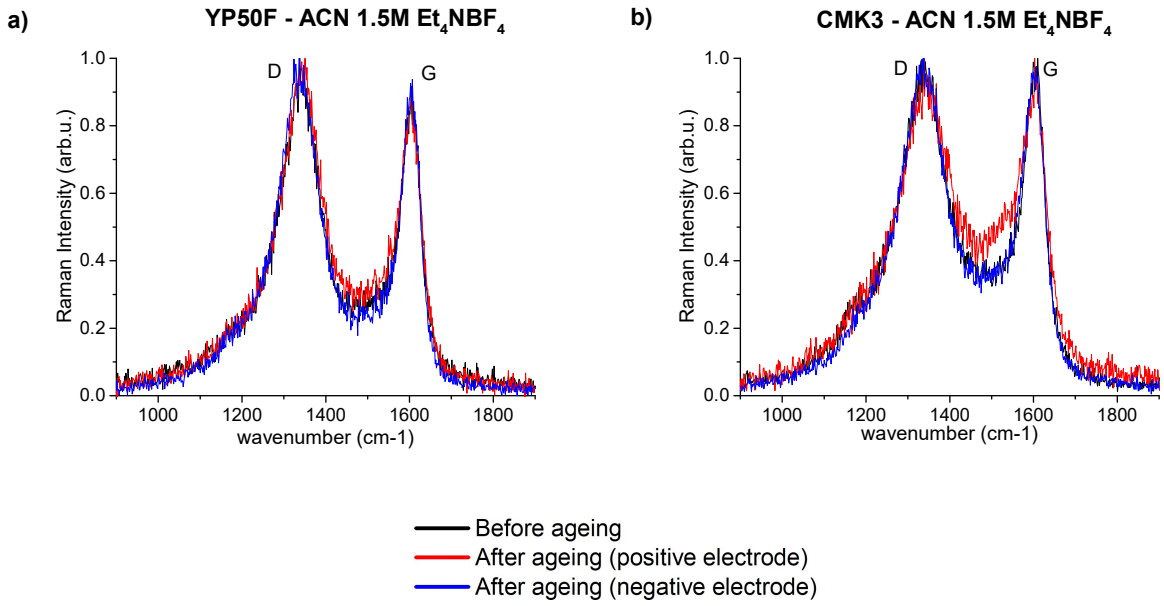

Figure 6: Raman spectra from YP50F material (a) and CMK3 material (b). Comparison between the before ageing electrode (black), negative electrode (blue) and positive electrode (red).

Electrode	Γ_{FWHM}(D) / cm^{-1}
CMK3 before aging	145
CMK3 negative (after aging)	136
CMK3 positive (after aging)	177
YP50F before aging	115
YP50F negative (after aging)	116

YP50F positive (after aging)	119

Table 1: Change of the full width at half maximum Γ_{FWHM} of the electrode before and after aging (positive and negative) for the two materials

To summarize Raman spectra information, electrochemical ageing of CMK3 positive electrode results in an increase of carbon defect density while the negative electrode remains the same, which well agrees with literature results[16]. This could be explained by resulting in the local oxidation of undercoordinated carbons or carbon defects. Differently, the YP50F positive electrode does not see any defect density increase after ageing.

According to TGA and Raman spectroscopy, both carbon-based electrodes experience an oxidation at the positive electrode. Together with gas sorption and EIS measurements, this suggests that the electrolyte is more likely to be involved for YP50F carbon positive electrode, leading to the formation of polymeric by-products clogging the microporosity. Differently, CMK3 positive electrodes seems to be oxidized and turns out to be more disordered after ageing. Regardless the porosity, the surface functional groups may play a role.

Figure 7 shows the evolution of $pH_{NaCl+carbon}$ versus pH_{NaCl} for YP50F (a) and CMK3 (b). We defined pH_{NaCl} as the pH of the NaCl solution, without carbon, $pH_{NaCl+YP50F}$ and $pH_{NaCl+CMK3}$ the pH of the solution NaCl with respectively YP50F and CMK3, measured after 12h.

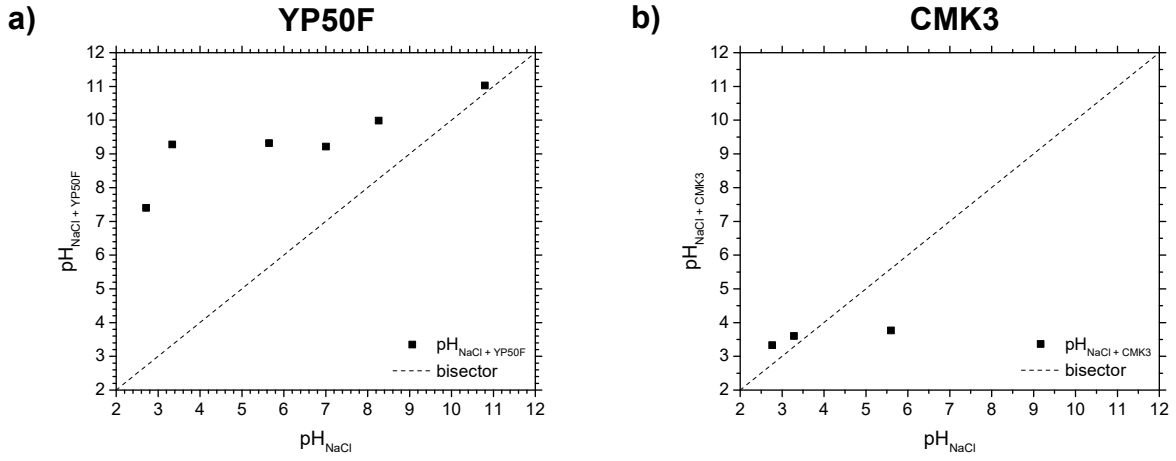

Figure 7: pH measurements of YP50F (a) and CMK3 (b). pH_{NaCl} is the pH value of the NaCl solution without carbon, $pH_{NaCl+carbon}$ is the pH value of the solution when carbon is instantly added.For YP50F, when carbon is added to the solution, $pH_{NaCl+YP50F}$ shift to basic values, compared to pH_{NaCl}. Those observations could be correlated with the hypothesis that YP50F have mainly a basic surface.

For CMK3, all solutions have a pH drop around 3 when the carbon is added. This acidic pH could be linked to acidic impurities between carbon grains, which could remain after the synthesis process.

To conclude on IEP measurements, observations of the pH variations are in line with the hypothesis of a basic surface for YP50F and an acidic surface for CMK3. However, it is important to highlight that the acidic surface of CMK3 could be due to synthesis impurities and maybe not surface functions.

Based on the above characterizations and observations, an ageing mechanism could be proposed for the two porous carbons (Figure 8).

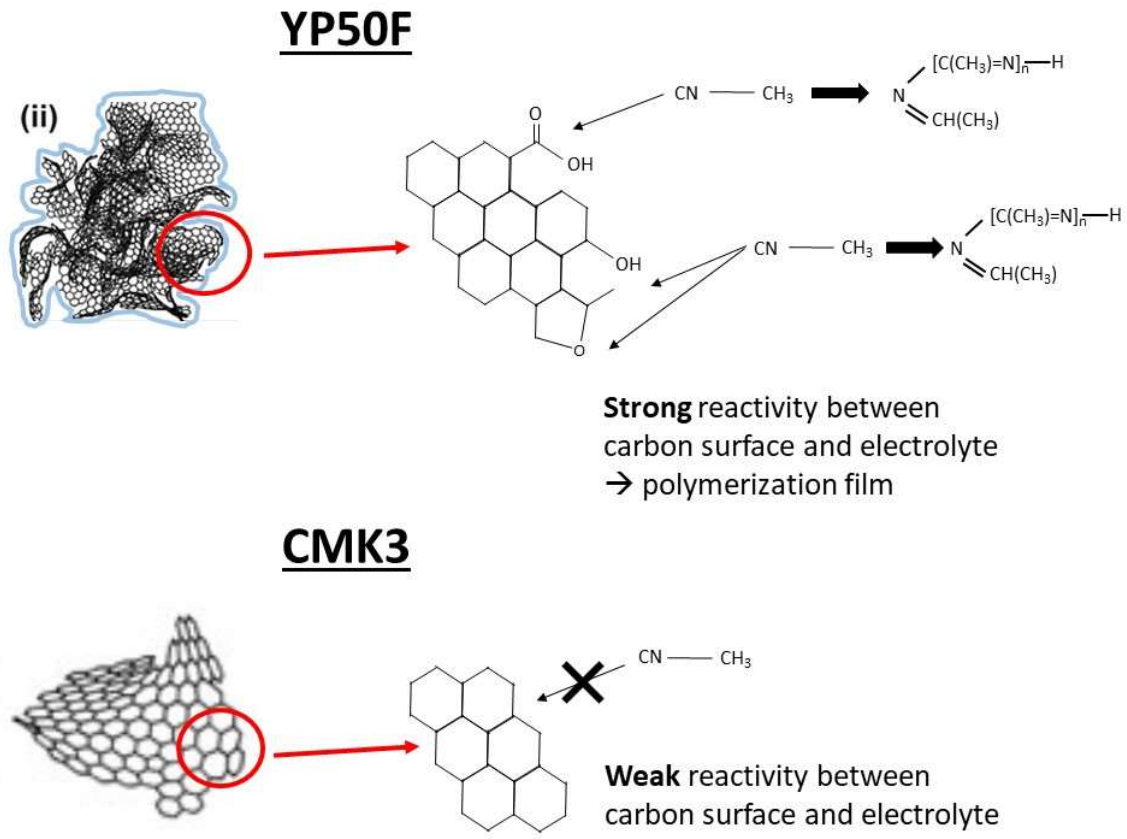

Figure 8: Proposed aged mechanism of YP50F and CMK3 in ACN - 1.5M Et_4NBF_4. Carbon structure was proposed by Terzyk et al. [30]. Polymerization film chemical nature was suggested by Liu et al.[31]

CONCLUSIONS

EDLC cells using porous carbons electrodes were assembled and aged in 1.5 M tetraethyl ammonium tetrafluoroborate (Et_4NBF_4) in acetonitrile (AN) electrolyte. Ageing of porous carbon-based electrochemical double layer cells were tested 1.5M Et_4NBF_4 in CH_3CN electrolyte. Two different porous carbons were employed, CMK3 (mesoporous carbon) and YP50F (microporous carbon). YP50F carbon was found to have a basic surface and CMK3 an acidic surface. However, CMK3 acidity could be due to synthesis process.

Electrochemical measurements showed that during the aging, capacitance and resistance felloff at the same rate for both carbons. Nevertheless, post-mortem impedance analysis showed CMK3 exhibit the same impedance diagram than before ageing, but shifted to more positive resistance, that may be due to a decrease of the carbon bulk electronic conductivity. On the other hand, YP50F impedance showed high frequency loop together with a decrease of the overall phase angle, both consistent with a degradation of the electrolyte-material interface, possibly caused by the formation of a polymerization film.[31]

TGA analyses showed the YP50F positive electrode exhibit a different thermal profile with mass losses occurring at lower temperatures, while no significant changes were observed for the YP50F negative electrode and for both the positive and negative CMK3 electrodes.

Gas sorption analyses of carbons after ageing revealed that positive electrode porous volume and specific surface area dropped drastically for both carbons, and micropores were found to be clogged in the YP50F carbon. Besides, Raman spectroscopy showed the mesoporous CMK3 carbon structure was more disordered after ageing, unlike observed for YP50F. According to those findings, it is reasonable to propose that CMK3 carbon is oxidized at the positive electrode upon ageing, while an electrolyte oxidation occurs at the YP50F positive electrode, resulting in carbon pore clogging. Moreover, IEP measurements revealed the presence of basic surface functions on YP50F carbon surface, which could easily react with the electrolyte during the ageing. It is likely that electrolyte degradation is preventing carbon oxidation, differently to CMK3.

ACKNOWLEDGMENT

We acknowledge funding from the French national agency of research. We also thank P. Puech (CEMES) for discussion on Raman analysis and Paolina Rozmus for her experimental work.

This research was funded, in whole or in part, by ANR, AAPG2019.

REFERENCES

(1) Simon, P.; Gogotsi, Y. Perspectives for Electrochemical Capacitors and Related Devices. *Nature Materials* **2020**, 13. https://doi.org/10.1038/s41563-020-0747-z.

(2) Gamby, J.; Taberna, P. L.; Simon, P.; Fauvarque, J. F.; Chesneau, M. Studies and Characterisations of Various Activated Carbons Used for Carbon/Carbon Supercapacitors. *Journal of Power Sources* **2001**, *101* (1), 109–116. https://doi.org/10.1016/S0378-7753(01)00707-8.

(3) Segalini, J.; Daffos, B.; Taberna, P.-L.; Gogotsi, Y.; Simon, P. Qualitative Electrochemical Impedance Spectroscopy Study of Ion Transport into Sub-Nanometer Carbon Pores in Electrochemical Double Layer Capacitor Electrodes. *Electrochimica Acta* **2010**, 7. http://dx.doi.org/10.1016/j.electacta.2010.01.003.

(4) Chmiola, J.; Yushin, G.; Gogotsi, Y.; Portet, C.; Simon, P.; Taberna, P. L. Anomalous Increase in Carbon Capacitance at Pore Sizes Less Than 1 Nanometer. *Science Magazine* **2006**, *313*, 5. http://dx.doi.org/10.1126/science.1132195.

(5) Fuertes, A. B.; Lota, G.; Centeno, T. A.; Frackowiak, E. Templated Mesoporous Carbons for Supercapacitor Application. *Electrochimica Acta* **2005**. https://doi.org/doi:10.1016/j.electacta.2004.11.027.

(6) Hahn, M.; Kotz, R.; Gallay, R.; Siggel, A. Pressure Evolution in Propylene Carbonate Based Electrochemical Double Layer Capacitors. *Electrochimica Acta* **2006**. https://doi.org/doi:10.1016/j.electacta.2006.01.080.

(7) Pameté, E.; Köps, L.; Kreth, F. A.; Pohlmann, S.; Varzi, A.; Brousse, T.; Balducci, A.; Presser, V. The Many Deaths of Supercapacitors: Degradation, Aging, and Performance Fading. *Advanced Energy Materials* **2023**, 2301008. https://doi.org/10.1002/aenm.202301008.

(8) Shafeeyan, M. S. A Review on Surface Modification of Activated Carbon for Carbon Dioxide Adsorption. *Journal of Analytical and Applied Pyrolysis* **2010**. https://doi.org/doi:10.1016/j.jaap.2010.07.006.

(9) Tanahashi, I.; Nishino, A. Effect Of Concentration Of Surface Acidic Functional Groups On Electric Double-Layer Properties Of Activated Carbon Fibers. **1989**. https://doi.org/10.1016/0008-6223(90)90062-4.

(10) Frackowiak, E. Carbon Materials for Supercapacitor Application. *Phys. Chem. Chem. Phy.* **2007**, *9*, 1774–1785. https://doi.org/10.1039/B618139M.

(11) Bittner, A. M. Ageing of Electrochemical Double Layer Capacitors. *Journal of Power Sources* **2012**. https://doi.org/doi:10.1016/j.jpowsour.2011.10.083.

(12) Yang, C.-H.; Nguyen, Q. D.; Chen, T.-H.; Helal, A. S.; Li, J.; Chang, J.-K. Functional Group-Dependent Supercapacitive and Aging Properties of Activated Carbon Electrodes in Organic Electrolyte. **2018**.

(13) Pourhosseini, S. E. M. Strategy to Assess the Carbon Electrode Modifications Associated with the High Voltage Ageing of Electrochemical Capacitors in Organic Electrolyte. *Energy Storage Materials* **2021**, 13.

(14) Cericola, D.; Ruch, P. W.; Foelske-Schmitz, A.; Weingarth, D.; Kötz, R. Effect of Water on the Aging of Activated Carbon Based Electrochemical Double Layer Capacitors During Constant Voltage Load Tests. *Int. J. Electrochem. Sci.* **2011**, *6*.

(15) Ma, N.; Yang, D.; Riaz, S.; Wang, L.; Wang, K. Aging Mechanism and Models of Supercapacitors: A Review. *Technologies* **2023**, *11* (2), 38. https://doi.org/10.3390/technologies11020038.
(16) Zhu, M.; Weber, C. J.; Yang, Y.; Konuma, M.; Starke, U.; Kern, K.; Bittner, A. M. Chemical and Electrochemical Ageing of Carbon Materials Used in Supercapacitor Electrodes. *Carbon* **2008**, *46* (14), 1829–1840. https://doi.org/10.1016/j.carbon.2008.07.025.
(17) Inagaki, M. Templated Mesoporous Carbons: Synthesis and Applications. **2016**. http://dx.doi.org/10.1016/j.carbon.2016.06.003.
(18) "Kuraray, YP50F Specifications," Can Be Found under Http://Www.Kuraraychemical.Com/Products/Sc/SCcarbon.Htm, n.d.
(19) Sun, X.; Zhang, X.; Huang, B.; Zhang, H.; Zhang, D.; Ma, Y. (LiNi0.5Co0.2Mn0.3O2 þ AC)/Graphite Hybrid Energy Storage Device with High Specific Energy and High Rate Capability. *Journal of Power Sources* **2013**, 8. https://doi.org/10.1016/j.jpowsour.2013.06.038.
(20) Liu, Y.; Soucaze-Guillous, B.; Taberna, P.-L.; Simon, P. Understanding of Carbon-Based Supercapacitors Ageing Mechanisms by Electrochemical and Analytical Methods. *Journal of Power Sources* **2017**, *366.*, 123-130. https://doi.org/10.1016/j.jpowsour.2017.08.104.
(21) Ruch, P. W.; Cericola, D.; Foelske-Schmitz, A.; Kã, R. Aging of Electrochemical Double Layer Capacitors with Acetonitrile-Based Electrolyte at Elevated Voltages. *Electrochimica Acta* **2010**. https://doi.org/doi:10.1016/j.electacta.2010.02.064.
(22) Mei, B.-A.; Munteshari, O.; Lau, J.; Dunn, B.; Pilon, L. Physical Interpretations of Nyquist Plots for EDLC Electrodes and Devices. *J. Phys. Chem. C* **2018**, *122* (1), 194–206. https://doi.org/10.1021/acs.jpcc.7b10582.
(23) Maurel, V. Operando AC In-Plane Impedance Spectroscopy of Electrodes for Energy Storage Systems. *Journal of The Electrochemical Society* **2022**.
(24) Azaıs, P.; Duclaux, L.; Florian, P.; Massiot, D.; Lillo-Rodenas, M.-A.; Linares-Solano, A.; Peres, J.-P.; Jehoulet, C.; Beguin, F. Causes of Supercapacitors Ageing in Organic Electrolyte. *Journal of Power Sources* **2007**, 8. https://doi.org/10.1016/j.jpowsour.2007.07.001.
(25) Silva, W. M.; Ribeiro, H.; Seara, L. M.; Calado, H. D. R.; Ferlauto, A. S.; Paniago, R. M.; Leite, C. F.; Silva, G. G. Surface Properties of Oxidized and Aminated Multi-Walled Carbon Nanotubes. *J. Braz. Chem. Soc.* **2012**, *23* (6).
(26) Bom, D.; Andrews, R.; Jacques, D.; Anthony, J.; Chen, B.; Meier, M. S.; Selegue, J. P. Thermogravimetric Analysis of the Oxidation of Multiwalled Carbon Nanotubes: Evidence for the Role of Defect Sites in Carbon Nanotube Chemistry. *Nano Lett.* **2002**, *2* (6).
(27) Tuinstra, F.; Koenig, J. L. Raman Spectrum of Graphite. https://doi.org/10.1063/1.1674108.
(28) Can, L. G.; Moutinho, M. V. O.; Lombardo, A.; Kulmala, T. S.; Ferrari, A. C. Quantifying Defects in Graphene via Raman Spectroscopy at Different Excitation Energies. *Nano Letters* **2011**, 7. https://doi.org/dx.doi.org/10.1021/nl201432g.
(29) Wu, T. Study on Raman Multi-Peak Fitting and Structure Quantitative Analysis of PAN-Based Carbon Fibers. *J Mater Sci* **2022**. https://doi.org/10.1007/s10853-022-07589-8.
(30) Terzyk, A. P.; Furmaniak, S.; Harris, P. J. F.; Gauden, P. A. How Realistic Is the Pore Size Distribution Calculated from Adsorption Isotherms If Activated Carbon Is Composed of Fullerene-like Fragments?W. **2007**.
(31) Liu, Y. Understanding Ageing Mechanisms of Porous Carbons in Non-Aqueous Electrolytes for Supercapacitors Applications. *Journal of Power Sources* **2019**.

SUPPLEMENTARY INFORMATION

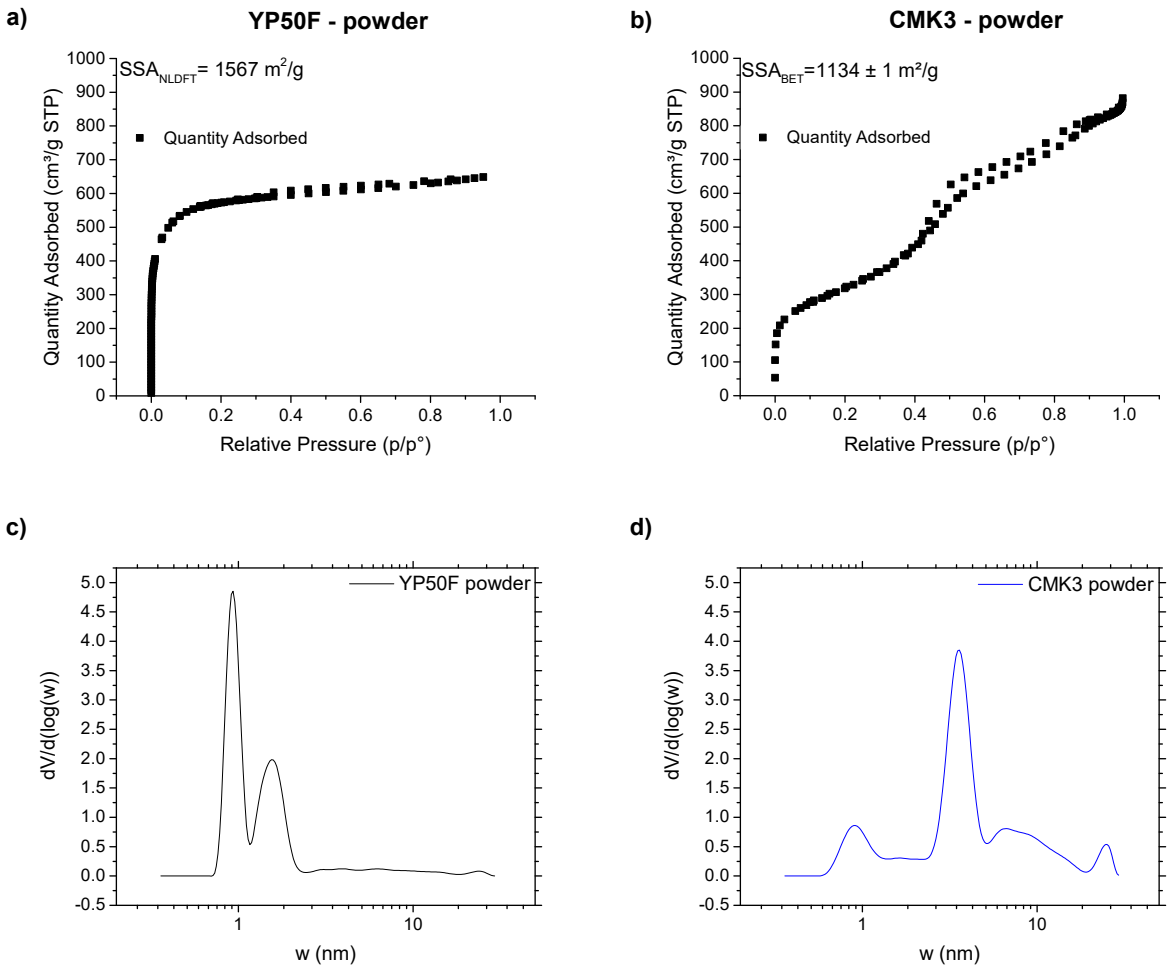

Figure S1: Gaz sorption experiments: isotherm of YP50F powder (a) and CMK3 powder (b), volume distribution of YP50F (c) and CMK3 (d).

Material	SSA ($m^2.g^{-1}$)	Porous volume ($cm^3.g^{-1}$)	Microporous Volume	Mesoporous volume
CMK3	(BET) 1134 ± 1	1.25	0.01 (1%)	1.24 (99%)
YP50F	(NLDFT) 1567	0.92	0.82 (90%)	0.10 (10%)

Table S1: SSA and porous volume ratios for CMK3 and YP50F carbons

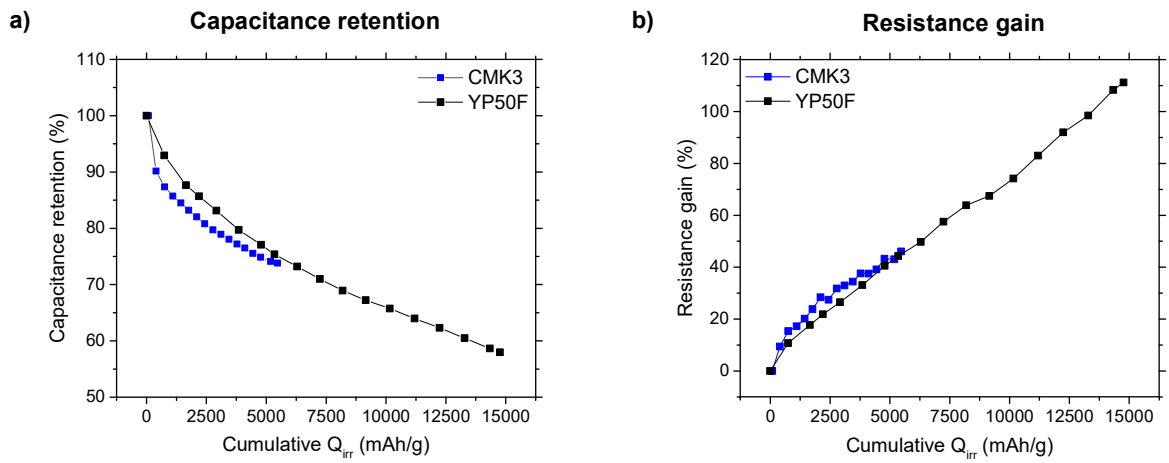

Figure S2: Evolution of capacitance (a) and resistance (b) versus the cumulative charge Q_{irr} (mAh/g) for YP50F and CMK3 in ACN 1.5M Et_4NBF_4

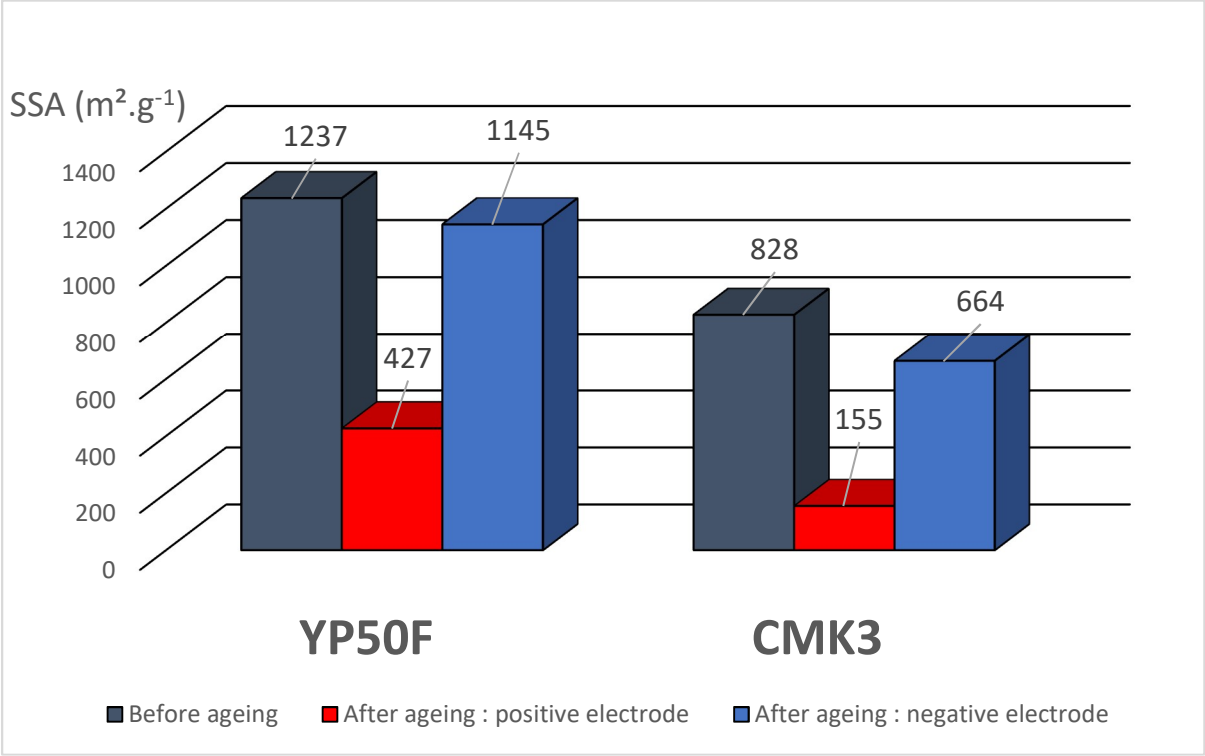

Figure S3: Change of the specific surface area (SSA) of the porous carbon electrodes before and after electrochemical ageing

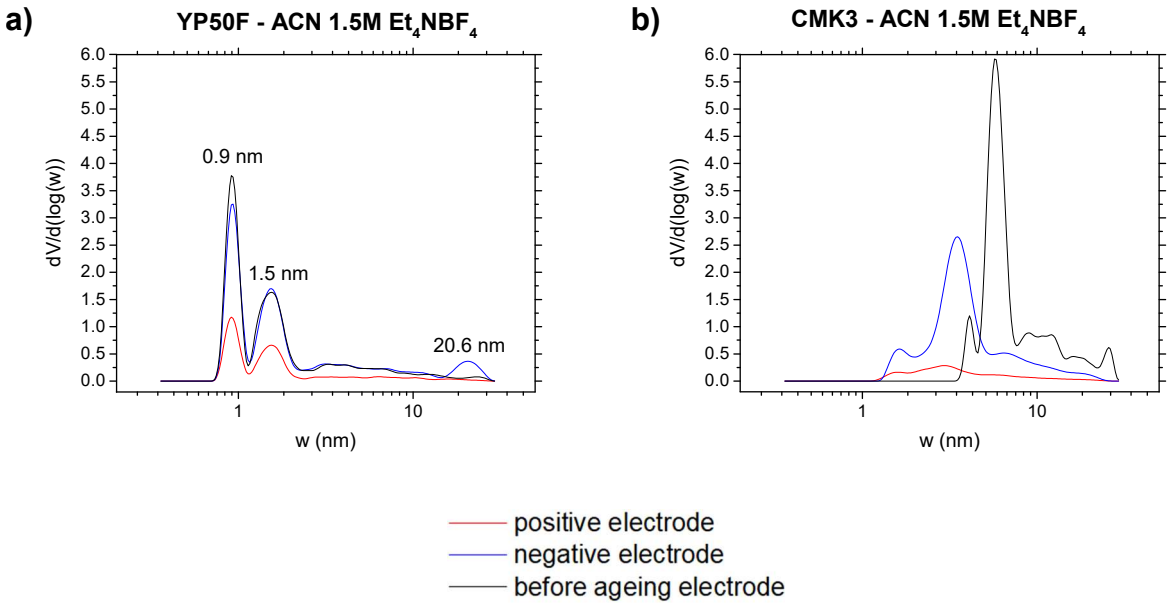

Figure S4: Volume distribution of microporosity (<2nm) and mesoporosity (2-50nm) for YP50F electrodes (a) and CMK3 electrodes (b).

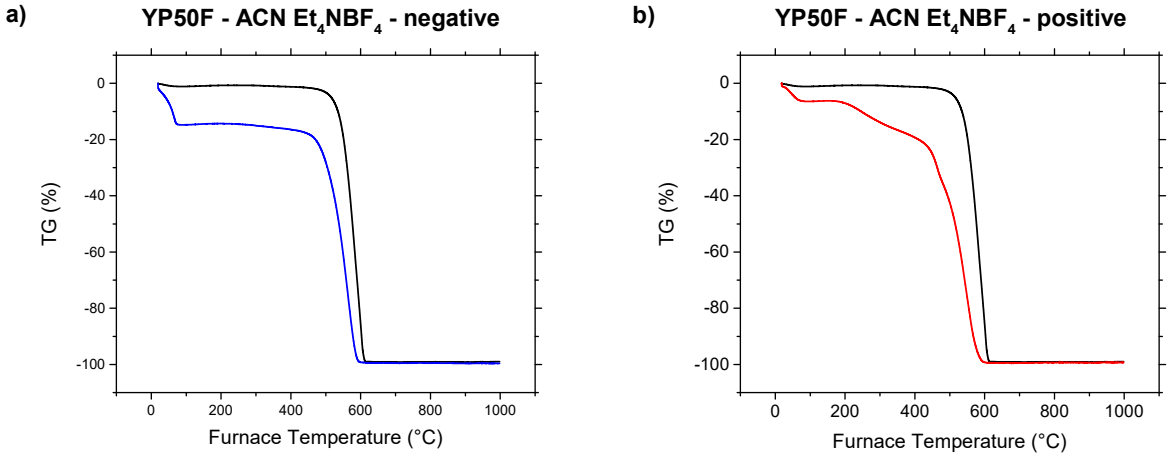

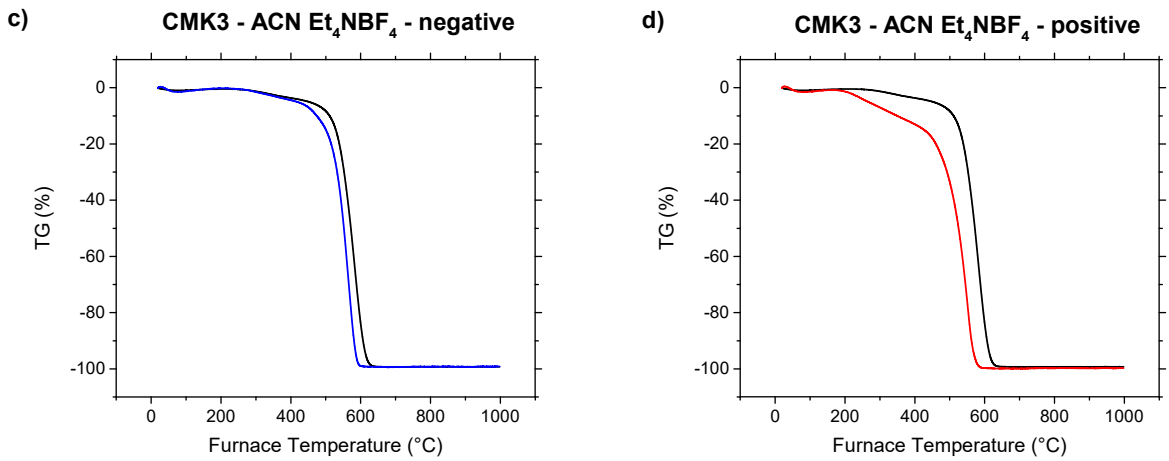

Figure S5: Thermograms of (a) YP50F after ageing negative electrode, (b) YP50F after ageing positive electrode (c) CMK3 after ageing negative electrode and (d) CMK3 after ageing positive electrode

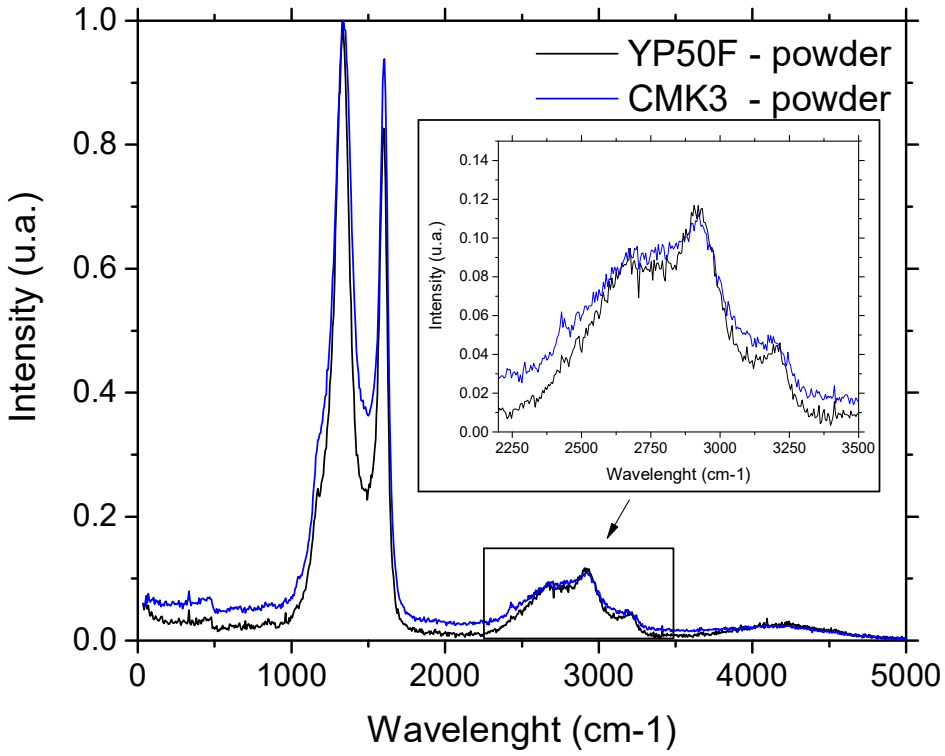

Figure S6: Raman spectra (reseau 600) with 2nd order pics for YP50F and CMK3 powders